The RoadMapping Code: How to deal with "Real World" Issues in Action-based Dynamical Modelling the Milky Way

W. Trick[1,2], J. Bovy[3,4], and H.-W. Rix[1]

trick@mpia.de

Subject headings: Galaxy: disk — Galaxy: fundamental parameters — Galaxy: kinematics and dynamics — Galaxy: structure

Contents

[1]Max-Planck-Institut für Astronomie, Königstuhl 17, D-69117 Heidelberg, Germany

[2]Correspondence should be addressed to trick@mpia.de.

[3]Institute for Advanced Study, Einstein Drive, Princeton, NJ 08540, USA

[4]Hubble fellow

1. Dynamical Modelling

1.1. Model

1.1.1. Actions

[TO DO]

1.1.2. Potential models

[TO DO: Mention different ways to calculate actions in different potentials.] [TO DO: Mention that the potential parameters are denoted by p_Φ]

1.1.3. Distribution function

Motivated by the findings of Bovy et al. 2012??? and Ting et al. (2013) about the simple phase-space structure of *MAP*s (see §**??**), and following Bovy & Rix (2013) and their successful application, we also assume that each *MAP* follows a single qDF of the form given by Binney & McMillan (2011). This qDF is a function of the actions $\boldsymbol{J} = (J_R, J_z, L_z)$ and

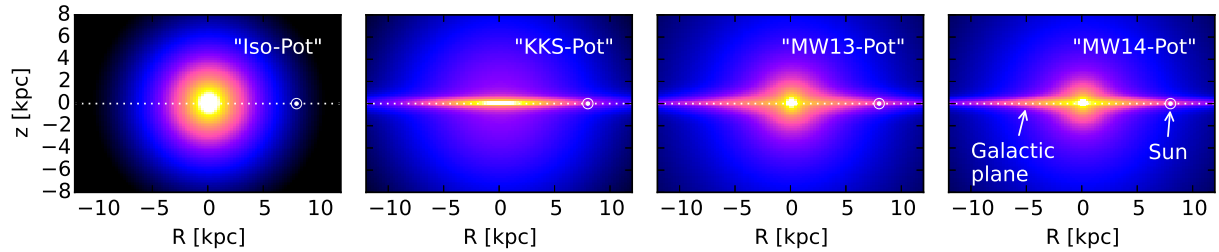

Fig. 1.— Density distribution of the four reference galaxy potentials in table 1, for illustration purposes. These potentials are used throughout this work for mock data creation and potential recovery. [TO DO: Halo sichtbarer machen, evtl. mit isodensity contours]

Table 1. Gravitational potentials of the reference galaxies used troughout this work and the respective ways to calculate actions in these potentials. All four potentials are axisymmetric. The potential parameters are fixed for the mock data creation. In the subsequent analyses we aim to recover these potential parameters again. All reference potentials assume the sun to be located at $(R_\odot, z_\odot) = (8\ \mathrm{kpc}, 0)$.

name	potential type	potential parameters p_Φ		action calculation	reference for potential type
"Iso-Pot"	isochrone potential	circular velocity at the sun	$v_{\mathrm{circ}} = 230\ \mathrm{km\ s^{-1}}$	***analytical and exact*** J_r, J_ϑ, L_z;	Binney & Tremaine (2008)
		isochrone scale length	$b = 0.9$ kpc	use $J_r \to J_R, J_\vartheta \to J_z$	
				in eq. (???)	
"KKS-Pot"	2-component	circular velocity at the sun	$v_{\mathrm{circ}} = 230\ \mathrm{km\ s^{-1}}$	***exact*** J_R, J_z, L_z	Batsleer & Dejonghe (1994)
	Kuzmin-Kutuzov-	focal distance of coordinate system[a]	$\Delta = 0.3$	using "Stäckel Fudge"	
	Stäckel potential	axis ratio of the coordinate surfaces[a] ...		(Binney 2012)	
	(disk + halo)	...of the disk component	$\left(\frac{a}{c}\right)_{\mathrm{Disk}} = 20$	and interpolation	
		...of the halo component	$\left(\frac{a}{c}\right)_{\mathrm{Halo}} = 1.07$	on action grid	
	(analytic potential)	relative contribution of the disk mass		(Bovy 2015)	
		to the total mass	$k = 0.28$		
"MW13-Pot"	MW-like potential with	circular velocity at the sun	$v_{\mathrm{circ}} = 230\ \mathrm{km\ s^{-1}}$	***approximate*** J_R, J_z, L_z	Bovy & Rix (2013)
	Hernquist bulge,	stellar disk scale length	$R_d = 3$ kpc	using "Stäckel Fudge"	
	2 exponential disks	stellar disk scale height	$z_h = 0.4$ kpc	(Binney 2012)	
	(stars + gas),	relative halo contribution to $v^2_{\mathrm{circ}}(R_\odot)$	$f_h = 0.5$	and interpolation	
	spherical power-law halo	"flatness" of rotation curve	$\frac{\mathrm{d}\ln(v_{\mathrm{circ}}(R_\odot))}{\mathrm{d}\ln(R)} = 0$	on action grid	
	(interpolated potential)			(Bovy 2015)	
"MW14-Pot"	MW-like potential with	-	-	***approximate*** J_R, J_z, L_z	Bovy (2015)
	cutoff power-law bulge,			(see "MW13-Pot")	
	Miyamoto-Nagai stellar disk,				
	NFW halo				

[a]The coordinate system of each of the two Stäckel-potential components is $\frac{R^2}{\tau_{i,p}+\alpha_p} + \frac{z^2}{\tau_{i,p}+\gamma_p} = 1$ with $p \in \{\mathrm{Disk}, /\mathrm{Halo}\}$ and $\tau_{i,p} \in \{\lambda_p, \nu_p\}$. Both components have the same focal distance $\Delta = \sqrt{\gamma_p - \alpha_p}$, to make sure that the superposition of the two components itself is still a Stäckel potential. The axis ratio of the coordinate surfaces $\left(\frac{a}{c}\right)_p := \sqrt{\frac{\alpha_p}{\gamma_p}}$ describes the flattness of the corresponding Stäckel component.

has the form

$$\begin{aligned}
\mathrm{qDF}(\boldsymbol{J} \mid p_{\mathrm{DF}}) &= f_{\sigma_R}\left(J_R, L_z \mid p_{\mathrm{DF}}\right) \times f_{\sigma_z}\left(J_z, L_z \mid p_{\mathrm{DF}}\right) && (1)\\
\text{with } f_{\sigma_R}\left(J_R, L_z \mid p_{\mathrm{DF}}\right) &= n \times \frac{\Omega}{\pi\sigma_R^2(R_g)\kappa}\left[1+\tanh\left(L_z/L_0\right)\right]\exp\left(-\frac{\kappa J_R}{\sigma_R^2(R_g)}\right) && (2)\\
f_{\sigma_z}\left(J_z, L_z \mid p_{\mathrm{DF}}\right) &= \frac{\nu}{2\pi\sigma_z^2(R_g)}\exp\left(-\frac{\nu J_z}{\sigma_z^2(R_g)}\right) && (3)\\
& && (4)
\end{aligned}$$

Here $R_g \equiv R_g(L_z)$ and $\Omega \equiv \Omega(L_z)$ are the (guidig-center) radius and the circular frequency of the circular orbit with angular momentum L_z in a given potential. $\kappa \equiv \kappa(L_z)$ and $\nu \equiv \nu(L_z)$ are the radial/epicycle (κ) and vertical (ν) frequencies with which the star would oscillate around the circular orbit in R- and z-direction when slightly perturbed (Binney & Tremaine 2008). The term $[1+\tanh(L_z/L_0)]$ suppresses counter-rotation for orbits in the disk with $L \gg L_0$ which we set to a random small value ($L_0 = 10 \times R_\odot/8 \times v_{\mathrm{circ}}(R_\odot)/220$).
For this qDF to be able to incorporate the findings by Bovy et al. 2012??? about the phase-space structure of *MAP*s summarized in §**??**, we set the functions n, σ_R and σ_z, which indirectly set the stellar number density and radial and vertical velocity dispersion profiles,

$$\begin{aligned}
n(R_g \mid p_{\mathrm{DF}}) &\propto \exp\left(-\frac{R_g}{h_R}\right) && (5)\\
\sigma_R(R_g \mid p_{\mathrm{DF}}) &= \sigma_{R,0} \times \exp\left(-\frac{R_g - R_\odot}{h_{\sigma_R}}\right) && (6)\\
\sigma_z(R_g \mid p_{\mathrm{DF}}) &= \sigma_{z,0} \times \exp\left(-\frac{R_g - R_\odot}{h_{\sigma_z}}\right). && (7)
\end{aligned}$$

The qDF for each *MAP* has therefore a set of five free parameters p_{DF}: the density scale length of the tracers h_R, the radial and vertical velocity dispersion at the solar position $R_\odot$, $\sigma_R, 0$ and $\sigma_z, 0$, and the scale lengths h_{σ_R} and h_{σ_z}, that describe the radial decrease of the velocity dispersion. The *MAP*s we use for illustration through out this work are summarized in Table 2.

One crucial point in our dynamical modelling technique (§???), as well as in creating mock data (§1.2), is to calculate the (axisymmetric) spatial tracer density $\rho_{\mathrm{DF}}(\boldsymbol{x} \mid p_\Phi, p_{\mathrm{DF}})$ for a given qDF and potential . We do this by integrating the qDF at a given (R, z) over all three

velocity components, using a $N_{\rm velocity}$-th order Gauss-Legendre quadrature for each integral:

$$\rho_{\rm DF}(R, |z| \mid p_\Phi, p_{\rm DF}) = \int_{-\infty}^{\infty} {\rm qDF}(\boldsymbol{J}[R, z, \boldsymbol{v} \mid p_\Phi] \mid p_{\rm DF})\, {\rm d}^3\boldsymbol{v} \tag{8}$$

$$\approx \int_{-N_{\rm sigma}\sigma_R(R|p_{\rm DF})}^{N_{\rm sigma}\sigma_R(R|p_{\rm DF})} \int_{-N_{\rm sigma}\sigma_z(R|p_{\rm DF})}^{N_{\rm sigma}\sigma_z(R|p_{\rm DF})} \int_0^{1.5 v_{\rm circ}(R_\odot)} {\rm qDF}(J[R, z, \boldsymbol{v} \mid p_\Phi] \mid p_{\rm DF})\, {\rm d}v_T\, {\rm d}v_z\, {\rm d}v_R, \tag{9}$$

where $\sigma_R(R \mid p_{\rm DF})$ and $\sigma_z(R \mid p_{\rm DF})$ are given by eq. (6) and (7) and the integration ranges are motivated by Fig. 2. For a given p_Φ and $p_{\rm DF}$ we explicitly calculate the density on $N_{\rm spatial} \times N_{\rm spatial}$ regular grid points in the (R, z) plane; in between grid points the density is evaluated with a bivariate spline interpolation. The grid is chosen to cover the extent of the observations for $z > 0$. The total number of actions that need to be calculated to set up the density interpolation grid is $N^2_{\rm spatial} \cdot N^3_{\rm velocity}$. Fig. ??? shows the importance of choosing $N_{\rm spatial}$, $N_{\rm velocity}$ and $N_{\rm spatial}$ sufficiently large in order to get the density with an acceptable numerical accuracy.

[TO DO: Rename everywhere $N_{\rm sigma}$ to $n_{\rm interval}$ or something like this.]

1.1.4. Selection function: observed volume and completeness

[TO DO]

Table 2. Reference distribution function parameters for the qDF in eq. (1)-(7). These qDFs describe the phase-space distribution of stellar *MAP*s for which mock data is created and analysed throughout this work for testing purposes. The parameters of the "cooler" ("hotter") *MAP*s were chosen such, that the they have the same σ_R/σ_z ratio as the "hot" ("cool") *MAP* . Hotter populations have shorter tracer scale lengths (Bovy et al. 2012d) and the velocity dispersion scale lengths were fixed according to Bovy et al. (2012c).

name of *MAP*	qDF parameters $p_{\rm DF}$				
	h_R [kpc]	σ_R [km s^{-1}]	σ_z [km s^{-1}]	h_{σ_R} [kpc]	h_{σ_z} [kpc]
"hot"	2	55	66	8	7
"cool"	3.5	42	32	8	7
"cooler"	2 +50%	55-50%	66-50%	8	7
"hotter"	3.5-50%	42+50%	32+50%	8	7

1.2. Mock Data

One goal of this work is to test how the loss of information in the process of measuring stellar phase-space coordinates can affect the outcome of the modelling. To investigate this, we assume first that our measured stars do indeed come from our assumed families of potentials and distribution functions and draw mock data from a given true distribution. In further steps we can manipulate and modify these mock data sets to mimick observational effects.
The distribution function is given in terms of actions and angles. The transformation $(\boldsymbol{J}_i, \boldsymbol{\theta}_i) \longrightarrow (\boldsymbol{x}_i, \boldsymbol{v}_i)$ is however difficult to perform and computationally much more expensive than the transformation $(\boldsymbol{x}_i, \boldsymbol{v}_i) \longrightarrow (\boldsymbol{J}_i, \boldsymbol{\theta}_i)$. We propose a fast and simple two-step method for drawing mock data from an action distribution function, which also accounts effectively for a given survey selection function.

Preparation: Tracer density. We first setup the interpolation grid for the tracer density $\rho(R, |z| \mid p_\Phi, p_{\mathrm{DF}})$ generated by the given qDF and according to §1.1.3 and Eq. 9. For the creation of the mock data we use $N_{\mathrm{spatial}} = 20$, $N_{\mathrm{velocity}} = 40$ and $N_{\mathrm{sigma}} = 5$.

Step 1: Drawing positions from the selection function. To get positions $\boldsymbol{x}_i$ for our mock data stars, we first sample random positions (R_i, z_i, ϕ_i) uniformly from the observed volume. Then we apply a rejection Monte Carlo method to these positions using the precalculated $\rho_{\mathrm{DF}}(R, |z| \mid p_\Phi, p_{\mathrm{DF}})$. In an optional third step, if we want to apply a non-uniform selection function, $\mathrm{sf}(\boldsymbol{x}) \neq$ const. within the observed volume, we use the rejection method a second time. The sample then follows

$$\boldsymbol{x}_i \longrightarrow p(\boldsymbol{x}) \propto \rho_{\mathrm{DF}}(R, z \mid p_\Phi, p_{\mathrm{DF}}) \times \mathrm{sf}(\boldsymbol{x}).$$

Step 2: Drawing velocities according to the distribution function. The velocities are independent of the selection function and observed volume. For each of the positions (R_i, z_i) we now sample velocities directly from the $\mathrm{qDF}(R_i, z_i, \boldsymbol{v} \mid p_{Phi}, p_{\mathrm{DF}})$ using a rejection method. To reduce the number of rejected velocities, we use a Gaussian in velocity space as an envelope function, from which we first randomly sample velocities and then apply the rejection method to shape the Gaussian velocity distribution towards the velocity distribution predicted by the qDF. We now have a mock data set according to the required:

$$(\boldsymbol{x}_i, \boldsymbol{v}_i) \longrightarrow p(\boldsymbol{x}, \boldsymbol{v}) \propto \mathrm{qDF}(\boldsymbol{x}, \boldsymbol{v} \mid p_\Phi, p_{\mathrm{DF}}) \times \mathrm{sf}(\boldsymbol{x}).$$

[TO DO: mention fig. 2. ???]

Introducing measurement errors. [TO DO]

[TO DO] Possible plots: *Diagram*: schematic flow chart of how to sample mock data (could be helpful for people, who want to sample mock data in action space and didn't know how to start, like me)

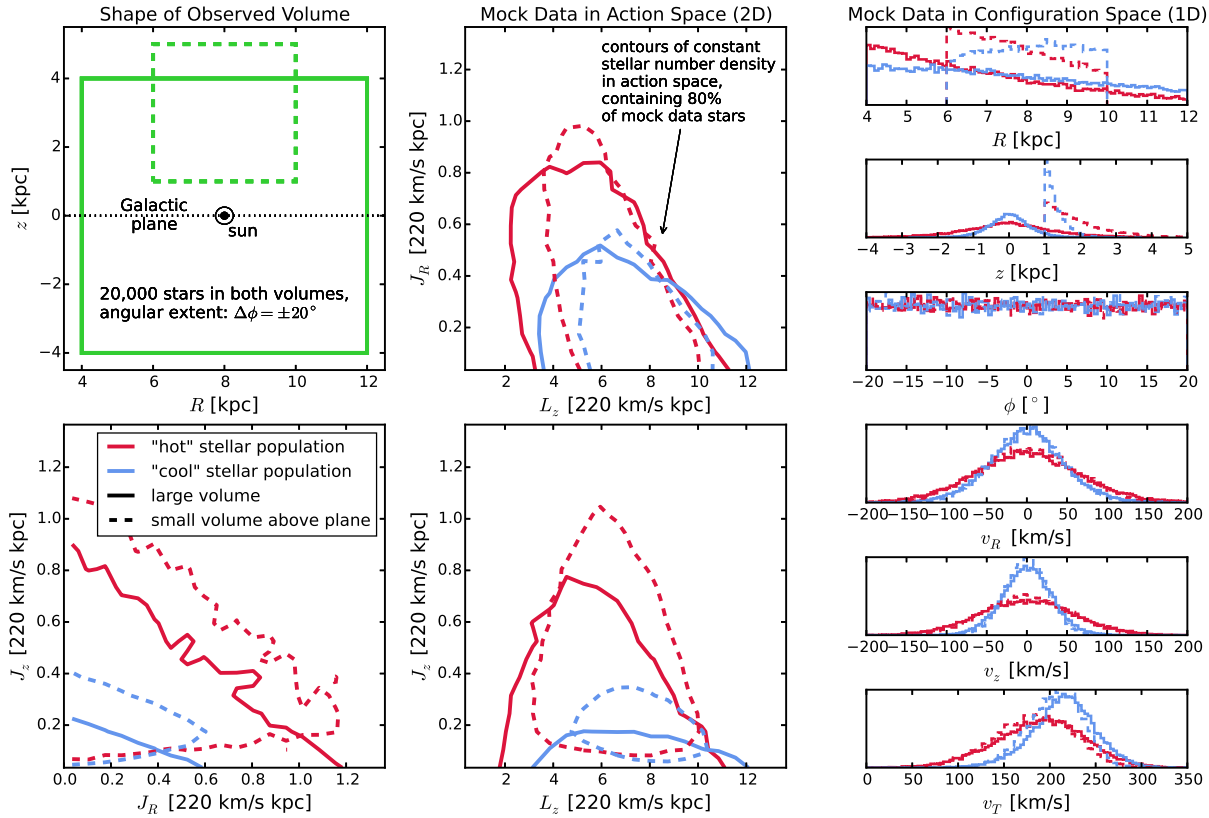

Fig. 2.— [TO DO: Rewrite caption] Distribution of mock data in action space (2D iso-density contours in the two central and the lower left panel) and configuration space (1D histograms in right panels), depending shape and position of observation volume (cf. lower left panel) and 'hottness' of the stellar population. The mock data was created in a 2-component KK-Staeckel-potential (cf. ???) with parameters $p_\Phi = \{v_{\rm circ}, \Delta, (a/c)_{\rm disk}, (a/c)_{halo}, k)\} = \{230 \text{ km s}^{-1}, 0.3, 20., 1.07, 0.28\}$ [TO DO: Does Δ have units????] (which is an approximate fit to the MilkyWay2014 potential in Galpy). We use two stellar populations, a 'hot' one with $p_{DF,hot} = \{h_R, \sigma_R, \sigma_z, h_{\sigma_R}, h_{\sigma_z}\} = \{2 \text{ kpc}, 55 \text{ km s}^{-1}, 66 \text{ km s}^{-1}, 8 \text{ kpc}, 7 \text{ kpc }\}$ (red lines) and a 'cool' population with $p_{DF,cool} = \{h_R, \sigma_R, \sigma_z, h_{\sigma_R}, h_{\sigma_z}\} = \{3.5 \text{ kpc}, 42 \text{ km s}^{-1}, 32 \text{ km s}^{-1}, 8 \text{ kpc}, 7 \text{ kpc }\}$ (blue lines). In the upper left panel we demonstrate the shape of the two different observation volumes within which we were creating each a 'hot' and a 'cool' mock data set: a large volume centered on the Galactic plane (solid lines in all plots) and a smaller one above the plane (dashed lines in all plots). Both volumes have an angular extent of $\Delta\phi \pm 20°$. Each of the four mock data sets compared in this plot has 20,000 stars in it. The stars of the 'cool' population have in general lower radial and vertical actions, i.e. are on more circular obrits. The different ranges of L_z's in the two volumes reflect $L_z \sim R v_{\rm circ}$ and the different radial extent of both volumes.The volume above the plane contains no stars with $J_z = 0$ and more with J_z: The higher a volume is located above the plane, the larger J_z has to be for the star's orbit to cross this volume. Circular orbits with $J_R = 0$ and $J_z = 0$ can obviously only be observed in the Galactic mid-plane. The smaller an orbit's L_z, the smaller also its mean orbital radius. For this orbit to be able to reach into a volume located at larger Galacto-centric radius, it needs to be more eccentric and therefore have a larger J_z. This anti-correlation between L_z and J_R can be seen in the top central panel. Orbits with both large J_R and large J_z would be very energetic and are therefore less likely to be observed. [TO DO: How many percent do the contours enclose????] [TO DO: redo with reference potential]

2. Results

2.1. What if our assumptions on the (in-)completeness of the data set are incorrect?

The selection function of a survey is described by a spatial survey volume and a completeness function, which determines the fraction of stars observed at a given location within the Galaxy with a given brightness, metallicity etc (see §[TO DO CHECK]). The completeness function depends on the characteristics and mode of the survey, can be very complex and is therefore sometimes not perfectly known. We investigate how much an imperfect knowledge of the selection function can affect the recovery of the potential. We model this by creating mock data with varying incompleteness, while assuming constant completeness in the analysis. The mock data comes from a sphere of $r_{\max} = 3$ kpc around the sun and an incompleteness function that drops linearly with distance r from the sun (fig. **??**):

$$\text{completeness}(r) = 1\epsilon_r \cdot \frac{r}{r_{\max}}$$

This could be understood as a model for the important effect of stars being less likely to be observed the further away they are. We demonstrate that the potential recovery with *RoadMapping* is very robust against somewhat wrong assumptions about the (in-)completeness of the data (see fig. **??**). A lot of information about the potential comes from the rotation curve measurements in the plane, which is not affected by applying an incompleteness function. In Appendix ??? we also show that the robustness is somewhat less striking but still given for small misjudgements of the incompleteness in vertical direction, parallel to the disk plane (fig. **??** and **??**). This could model the effect of wrong corrections for dust obscurement in the plane. We also investigate in Appendix ??? if indeed most of the information is stored in the rotation curve. For this we use the same mock data sets as in fig. **??** and **??**, but this time were not including the tangential velocities in the modelling, rather marginalizing the likelihood over v_T. In this case the potential is much less tightly constrained, even for 20,000 stars. For only small deviations of true and assumed completeness ($\lesssim 10\%$) we can however still incorporate the true potential in our fitting result (see fig. ???).

Stuff that needs to be further examined:

[TO DO] Maybe instead of decreasing completeness with height above the plane, a completeness that INcreases with height above the plan, to model e.g. obscuration due to dust.

[TO DO] Make similar test as isoSphFlexIncompR, but with KKS potential, to test, if this robustness is a special case for the isochrone potential.

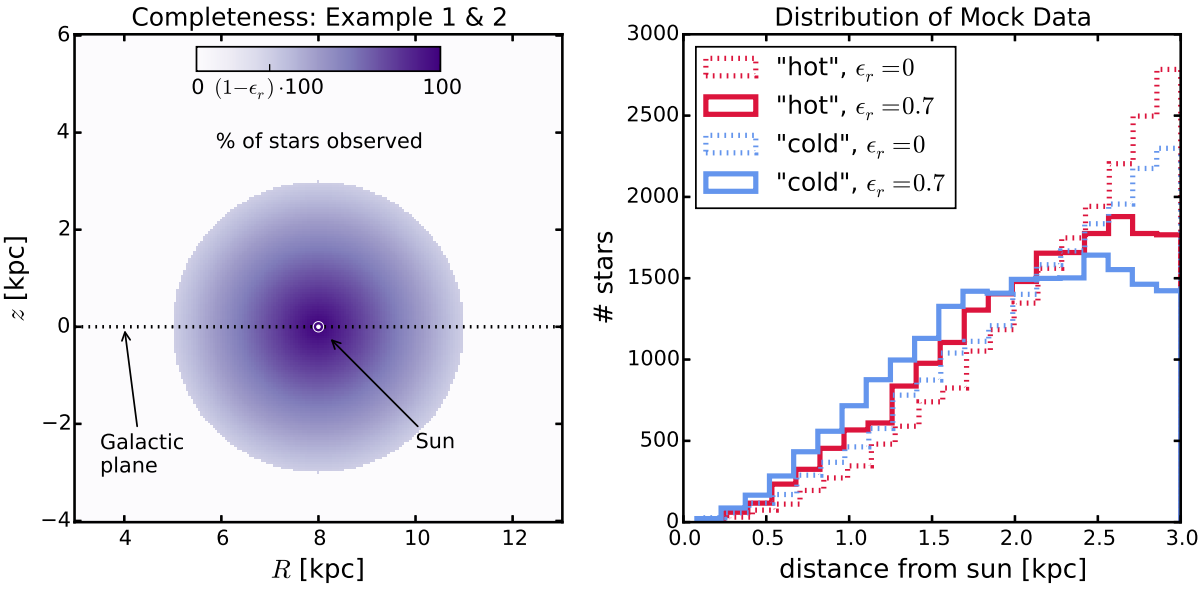

Fig. 3.— [TO DO: Rewrite caption] Selection function and mock data distribution for investigating radial (Example 1 & 2, left) and vertical (Example 3 & 4, right) incompleteness of the data. The survey volume is a sphere around the sun with $r_{\rm max} = 3$ kpc. In Example 1 & 2 (Example 3 & 4) the percentage of observed stars is decreasing linearly with radius from the sun (height above the Galactic plane), as demonstrated in the first row of panels. How fast this detection rate drops is quantized by the factor ϵ_r (ϵ_z) in eq. (**??**) (eq. (**??**)). Different mock data sets have different ϵ_r (ϵ_z). Histograms for four data sets, each with 20,000 and drawn from two *MAP*s ("hot" in red and "cool" in blue, see table 2) and with two different ϵ_r (ϵ_z), 0 and 0.7, are shown in the lower two panels for illustration purposes.[TO DO: Re-do, if new analyses are in violin plot.]

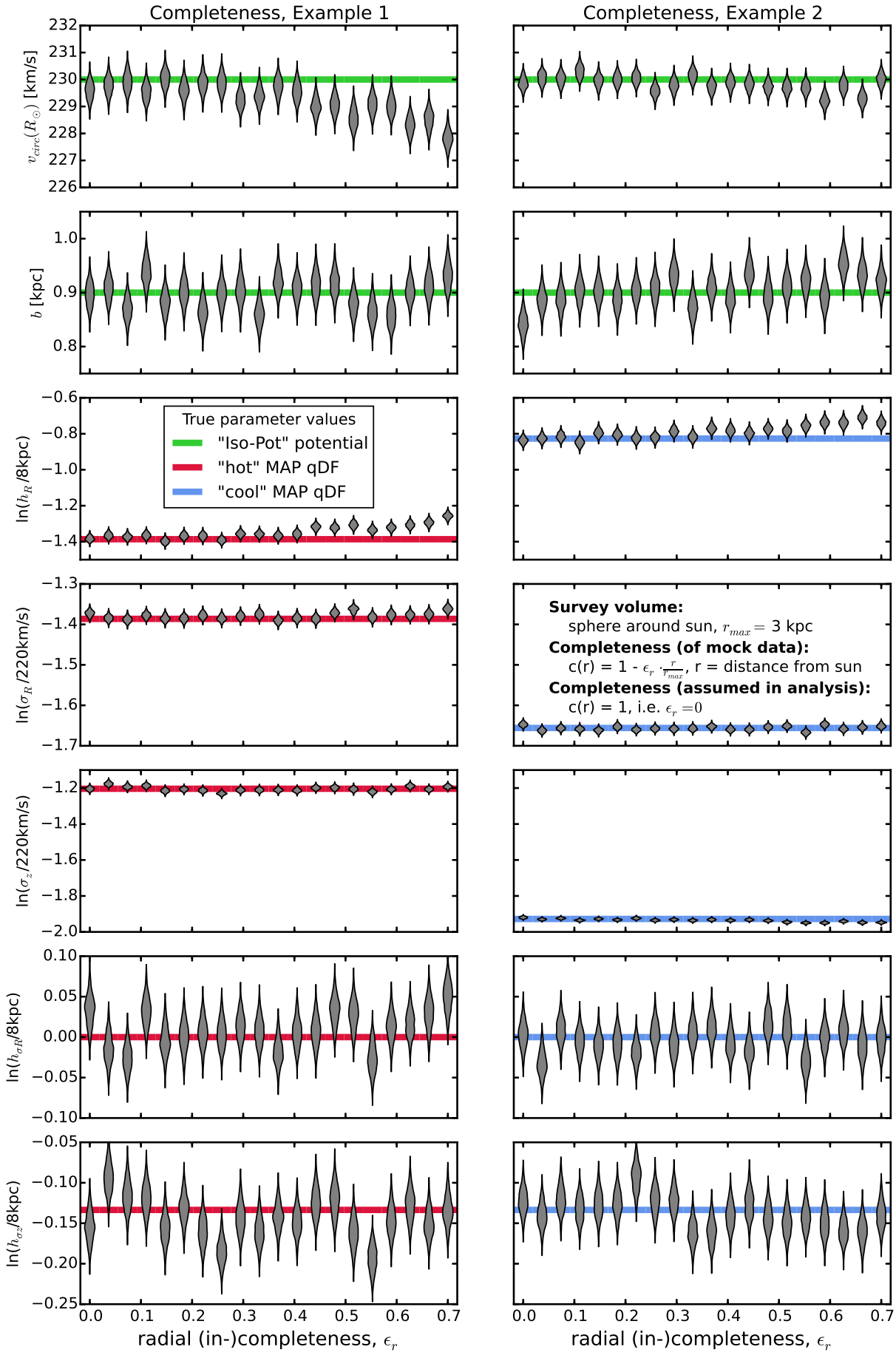

Fig. 4.— Caption [TO DO] (This was done using the current qDF to set the fitting range.

A. Appendix

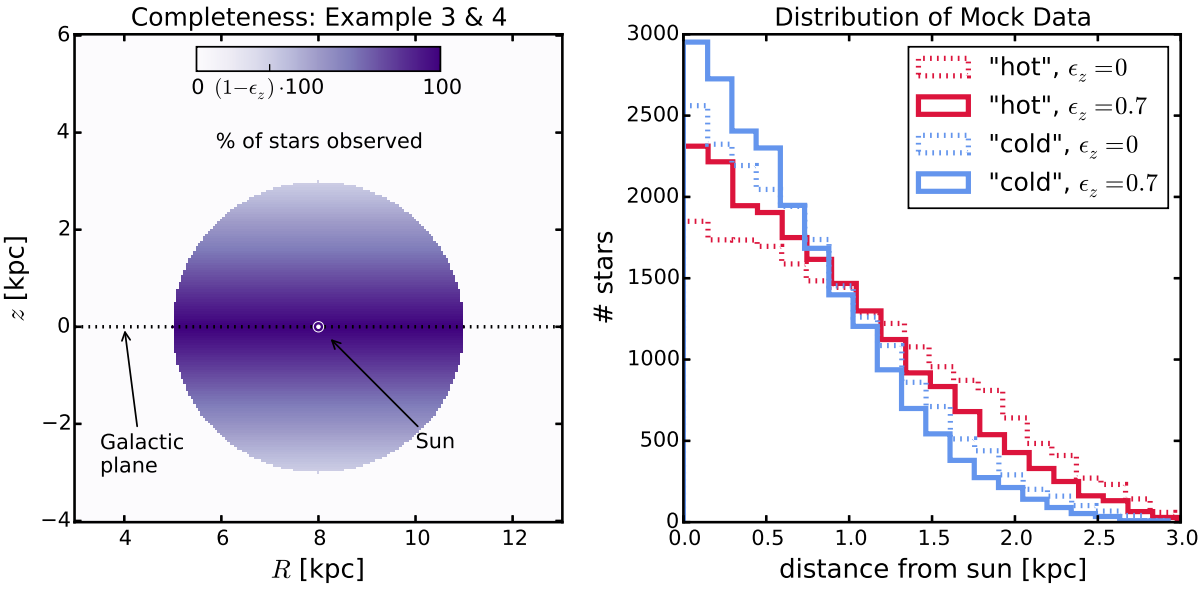

Fig. 5.— [TO DO: Rewrite Caption] Selection function and mock data distribution for investigating radial (Example 1 & 2, left) and vertical (Example 3 & 4, right) incompleteness of the data. The survey volume is a sphere around the sun with $r_{\rm max} = 3$ kpc. In Example 1 & 2 (Example 3 & 4) the percentage of observed stars is decreasing linearly with radius from the sun (height above the Galactic plane), as demonstrated in the first row of panels. How fast this detection rate drops is quantized by the factor ϵ_r (ϵ_z) in eq. (**??**) (eq. (**??**)). Different mock data sets have different ϵ_r (ϵ_z). Histograms for four data sets, each with 20,000 and drawn from two *MAP*s ("hot" in red and "cool" in blue, see table 2) and with two different ϵ_r (ϵ_z), 0 and 0.7, are shown in the lower two panels for illustration purposes.[TO DO: Re-do, if new analyses are in violin plot.]

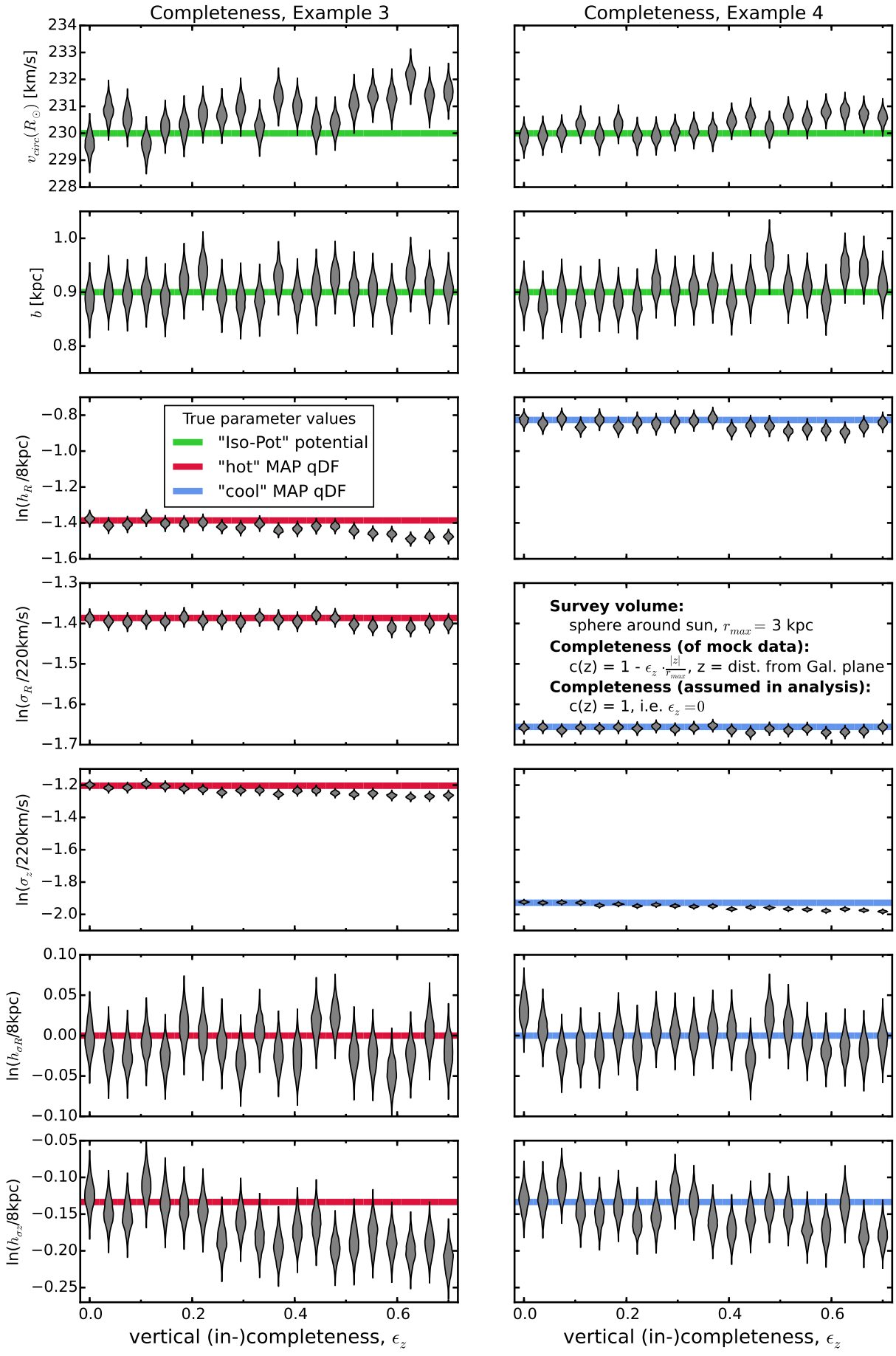

Fig. 6.— Caption [TO DO] (This was done using the current qDF to set the fitting range.

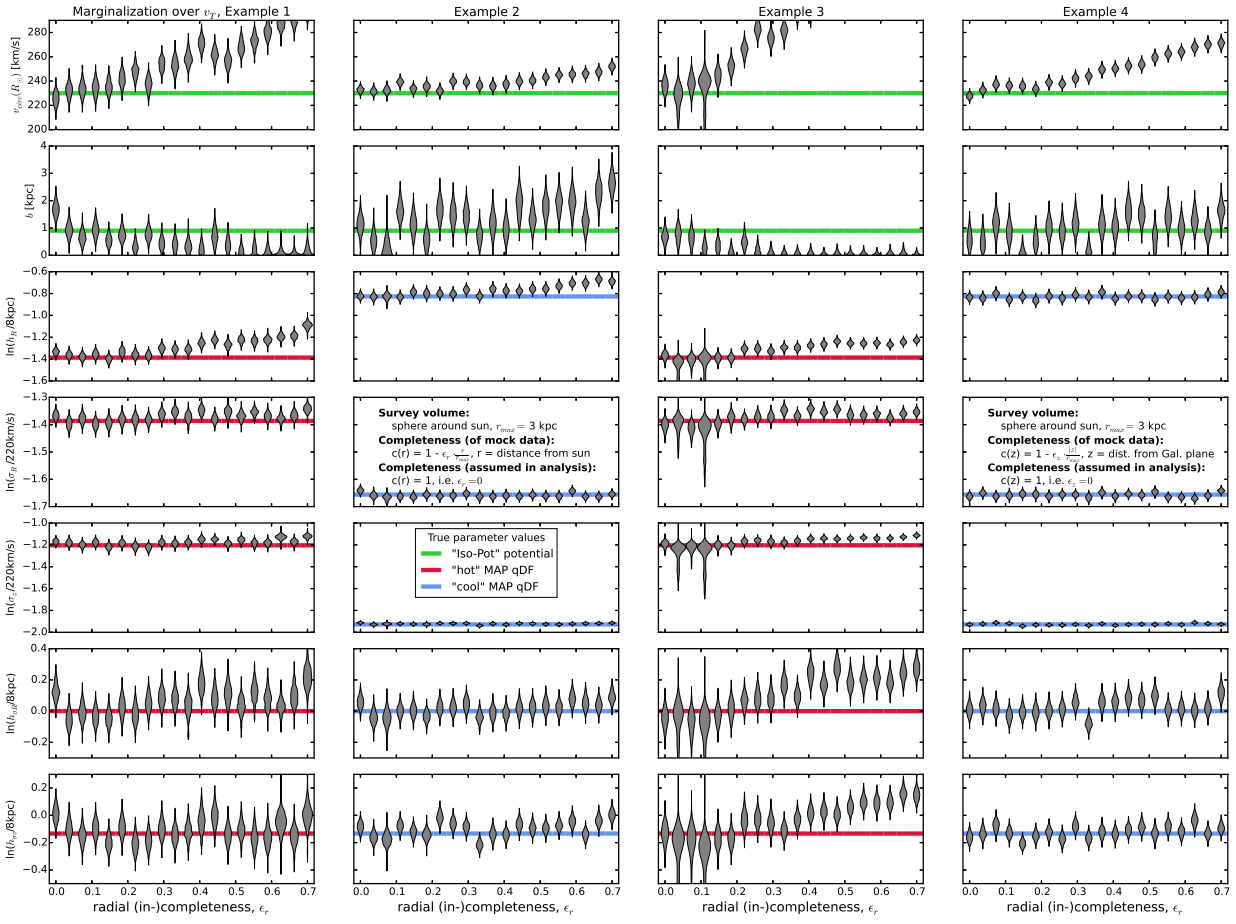

Fig. 7.— Caption [TO DO] ([TO DO: Redo all analyses for which MCMC did not converge to expected peak, and for which b ¡0 was not excluded. ???])

2. Questions that haven't been covered so far:

- What limits the overall code speed?
- What happens, when the errors are not uniform?
- What if errors in distance matter for selection?
- Deviations from axisymmetry: Take numerical simulations.

[TO DO: Check if all references are actually used in paper. ???]

REFERENCES

[TO DO]

Binney, J. J., & McMillan, P. 2011, MNRAS, 413, 1889

Binney, J. J. 2012, MNRAS, 426, 1324

Bovy, J., Rix, H.-W., & Hogg, D. W. 2012b, ApJ, 751, 131

Bovy, J., Rix, H.-W., Hogg, D. W. et al., 2012c, ApJ, 755,115

Bovy, J., Rix, H.-W., Liu, C. et al., 2012d, ApJ, 753, 148

Bovy, J., & Rix, H.-W. 2003, ApJ, 779, 115

Piffl, T., Binney, J., & McMillan, P. J. et al., 2014, MNRAS, 455, 3133

Steinmetz, M. et al., 2006, AJ, 132, 1645

Ting, Y.-S., Rix, H.-W., Bovy, J., & van de Ven, G. 2013, MNRAS, 434, 652

Binney, J., & Tremaine, S. 2008, [TO DO: Galactic Dynamics???]

[TO DO] Sanders & Binney (2015) Extended distribution functions for our Galaxy

[TO DO] Bovy (2015) Galpy paper